

## SIZE AND GEOMETRY EFFECTS

S. Banerjee

*Metallurgical Engineering, Indian Institute of Technology, IIT Powai, Bombay 400076, India*

### ABSTRACT

This paper discusses analytical and experimental results which show that plastic zone size in a precracked body with given aspect ratio, is mildly dependent on thickness and decreases as the width increases. The import of these results in the determination of fracture toughness and in the studies related to fatigue crack growth are discussed. A new procedure for the determination of size-independent fracture toughness is proposed and verified. The problems relating to a reliable characterization of size- and geometry-independent fatigue crack growth rate are briefly discussed.

### KEYWORDS

Plasticity, plastic zone, displacement, size, geometry, fracture toughness, fatigue crack growth rate, closure, plastic energy dissipation.

### INTRODUCTION

The effect of size and geometry on fracture and fatigue of precracked bodies is important due to two obvious reasons. First, all fracture mechanics based tests, analyses and design are founded on the premise that the fracture or the fatigue behaviour of a specimen tested in the laboratory simulates the corresponding behaviour of a real world structure even though (i) the size of a structure is, often, orders of magnitude larger than the specimen, and (ii) the geometries of the two are entirely different. Thus, the effect of size and geometry should be suitably characterized in order to produce a reliable fracture or fatigue safe design. Secondly, a meaningful fracture or fatigue behaviour of a material should be independent of size and geometry and should depend only on the material with a given microstructure. This aspect is important in order to understand

the origin of toughness and to develop materials with higher fracture and fatigue resistance.

The various fracture events like the start of crack extension, stable crack growth or unstable crack extension, and the fatigue crack growth are controlled by the stresses or strains very near to the crack tip. The near-tip stresses or strains are, in turn, predominantly determined by the singularity. Fracture mechanics parameter, the stress intensity factor,  $K$ , represents only the  $1/\sqrt{r}$  type singular stress term and the contribution of the non-singular stresses are assumed to be negligible. However, the non-singular stress is not always insignificant and its magnitude depends on dimensions such as crack length, the ligament and also the geometry of the precracked body. Accordingly, the actual stresses at the crack tip could depend on these factors. Therefore, in order that  $K$  faithfully represents the stresses or strains near the crack tip and thereby correctly characterizes the various fracture and fatigue events, the differences between the actual stresses and the stresses as represented by  $K$  in the neighbourhood of the crack tip, should be less than a permissible maximum. This maximum is assumed to be 5%. (Chona, Irwin and Sanford, 1983). The difference between the actual stresses and the stresses represented by  $K$  in any given geometry decreases with increasing size of crack length and ligament.

An appraisal of this difference at various points ahead of the crack tip was made using boundary collocation (Wilson, 1967). This difference for the CT is more than that for the CCT geometry. At small values of  $r/a$ , that is at large 'a' and small values of  $r$ , the difference decreases and, therefore,  $K$  characterizes the stresses near the crack tip with a better accuracy. If one considers  $r$  as the fracture process size, then  $r$  is the distance over which the fracture event is localized; in a brittle material, obviously  $r$  is small; less than few tens of microns. Therefore, in such a material,  $K$  can satisfactorily characterize a fracture or fatigue event, even when 'a' and  $(W-a)$  of the specimen are small. The other fracture mechanics parameters such as  $J$  or COD are related to  $K$  in the linear elastic regime and they too would exhibit similar behaviour.

Recently, photoelastic technique (Chona, Irwin and Sanford, 1983) have been used to determine the contribution of non-singular terms to the actual stresses, and the size of the singularity-dominated region in different fracture test specimen geometries. The study shows that the size of the singularity dominated region and the contribution of the non-singular terms to the actual crack tip stresses during fracture toughness testing varies with geometry and also dimensions such as  $W$  and  $a$ . In order that  $K$  yields a satisfactory approximation of the exact elastic stress field, the authors suggest that plasticity crack size adjustment should be less than the size of singularity dominated region during fracture toughness testing.

The situation discussed above is complicated by the inevitable formation of plastic zone at the crack tip. It is conventionally argued using reasons similar to that stated above that as long as the plastic zone is small compared to the dimensions of a

precracked body, the plastic zone size is hardly influenced by the far field stresses or in other words, by the size and geometry of the precracked body. This is referred to as small scale yielding situation and the plastic zone,  $R$ , in such a case is given by

$$R = \frac{1}{m\pi} \left( \frac{K}{\sigma_Y} \right)^2 \quad (1)$$

where  $\sigma_Y$  is uniaxial yield strength and  $m$  is a constant which is assumed to be equal to 1 for plane stress and 3 for plane strain. However, as shown later in this paper,  $R$  at a given  $K$  and  $\sigma_Y$  can depend on  $W$ ,  $a$  and specimen geometry even when  $R$  is smaller than the plastic zones normally permitted in the  $K_{IC}$  test procedures of ASTM E399 or the fatigue crack growth rate determination procedure of ASTM E647. This result has important consequences in the practical problems of fatigue and fracture. The objective of this paper is to present these results and to examine the import of these results in the determination of fracture toughness and in the studies related to fatigue crack growth.

#### ANALYTICAL RESULTS ON SIZE AND GEOMETRY DEPENDENT PLASTICITY

The plasticity in a precracked body can be evaluated in terms of plastic zone size or in terms of the displacement produced by growth of plastic zone. The measurement of plastic zone is not easy. On the other hand, the resultant displacement can be measured with less difficulty and compared with analytical results.

The formation of plastic zone in finite precracked bodies has been studied by several investigators using either the Dugdale (1960) model or the finite element method. In addition, a somewhat unconventional procedure based on the stress distribution in the ligament of a precracked specimen has also been used to calculate the plastic zone size and displacement. The results based on these three approaches are discussed subsequently.

##### Dugdale Model

Heald, Spink and Worthington (1972) noted that the Dugdale model does not account for the effect of geometry or shape of the structure on the plastic zone size and accordingly introduced a suitable correction factor to modify the model. de Wit (1983) has used this modified model to define the boundaries of three different categories of failure: linear elastic, elastic-plastic and collapse; and correlated them with other failure criteria which are verified by experimental data.

Recently, Terada (1983) and Mall and Newman (1984) applied Dugdale model to calculate plastic zone size in CT specimen geometry using the collocation technique. The results of these two investigations are in excellent agreement.

Terada has contended that the plastic zone size calculated in the CT specimen, agrees reasonably well with the predictions

of equation (1) for plane strain condition where value of  $m$  is assumed to be equal to 3. However, as discussed below, the observed agreement may be fortuitous. For, Dugdale solution is essentially a plane stress solution and therefore it would be more appropriate to compare the results of Dugdale analysis with the prediction of equation (1), wherein the value of  $m$  is 1. There is a more important point, Terada's (1983) results on CT specimen using Dugdale's plasticity give displacement values which are unusually large compared to the experimentally measured displacement values. While only a few experimental displacement values are reported in the literature, the 5% secant  $K_Q$  values of ASTM E399 for CT specimen have been determined in situation where crack extension is absent. These experimental  $K_Q$  values are twice as large as that predicted by Terada's (1983) results of Dugdale's analysis; this is expected, since Dugdale's analysis is for plane stress situation. Therefore, these results of Dugdale's analysis on CT specimen can give qualitative guidelines but they cannot be directly used to predict the effect and role of size dependent plasticity in the determination of fracture toughness and characterization of fatigue crack growth.

Fuhring and Seeger (1979) have reported solution for Dugdale's plastic zone for an infinite array of collinear cracks. Plastic zone determined from this solution differs from that obtained from Terada's solution for CT specimen. The difference in plastic zone size is significant even when the plastic zones are rather small.

Calculations from the solution (Fuhring and Seeger, 1979), also show that plastic zone size is significantly size dependent. For example, for a  $K/\sigma_y$  value as low as 0.1 m and  $a/W = 0.1$ , an order of magnitude increase in  $w$ , decreases the plastic zone size by about 2.5 times. Thus, the usual difference in size between the specimen and structure may produce significant difference in crack tip plastic zone even when the plastic zones are relatively small. At higher  $K/\sigma_y$  values, the difference could be significantly larger.

#### Finite Element

Finite element analysis (Larsson and Carlsson, 1973) shows that there is a significant difference in the plastic zone of a CT and CCT specimen. In an unpublished work, similar difference has also been observed between CCT and SENT specimen, wherein the plastic zone in CCT specimen is larger than that observed in SENT specimen (Rajendran and Banerjee, 1984). In this investigation, finite element analysis has also been used to determine plastic zone in two CCT specimens with identical  $a/W$  and mesh configuration, but the width and other related dimensions of one are five times those of the other. The results show that in case of a CCT specimen, an increase in  $W$ , decreases plastic zone size.

Small scale yielding plastic zone size and shape determined through finite element and other methods has earlier been compared with the experimentally determined plastic zone size and

shape (Broek, 1978). The agreement is not satisfactory as regards the plastic zone shape. This is not surprising in view of the results discussed above and also in view of the inherent difficulties in the experimental determination of plastic zone size. It is more convenient to compare the displacement values produced by plasticity.

The displacement produced by the growth of plastic zone has been obtained from finite element. The results obtained for plain strain condition yield displacement values which are smaller (Banerjee, 1981) and  $K_Q$  values which are significantly higher, than those observed by experiments (Munz, 1977, 1979, Banerjee, 1981). On the other hand, it is expected that the results obtained for plane stress condition would exhibit an opposite trend. The reason is that the actual experimental value corresponds to a three dimensional elastic-plastic state of stress and to the author's knowledge this problem is yet to be satisfactorily solved.

#### An Approximate And Simple Method

As against the Dugdale's analysis and the finite element method discussed above, an approximate but simple method of determination of plastic zone has been developed and reported elsewhere (Paranjpe, 1977, Paranjpe and Banerjee, 1977, Banerjee, 1981). The result obtained from this analysis is reported in the form of plots: (i) plastic flow curve and (ii) dependence of plastic zone size. Fig. 1 reports the plastic flow curve for CT, TPB and SENT geometry. Such results have also been obtained for other  $a/W$  values. The plastic flow curve reported here for the CT specimen is compared subsequently with the experimental plastic flow curve. On the other hand, Fig. 2 reports the plastic zone size as dependent on  $W$  for CT specimens with different  $a/W$  values.

The analytical results discussed thus far, refer to the growth of plastic zone under mode I loading. However, a circumferentially cracked round bar subjected to torsion and which corresponds to mode III loading produces a plastic zone which depends on the crack depth and the diameter of the bar. At a given aspect ratio, the larger the diameter, smaller the plastic zone. Plastic flow curves generated analytically for the mode III loading have been compared later, with the experimentally determined plastic flow curves.

#### EXPERIMENTAL OBSERVATION OF SIZE DEPENDENT PLASTICITY

The evidence of size dependent plasticity is obtained from four experimental observations:

1. Plastic flow curve
2. Near tip contraction
3.  $K_Q$  values
4. Plastic zone size determined through the observation of out of plane contraction.

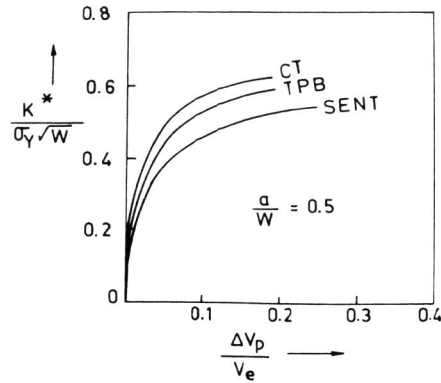


Fig. 1. Plastic flow curves for specimens of different geometries.

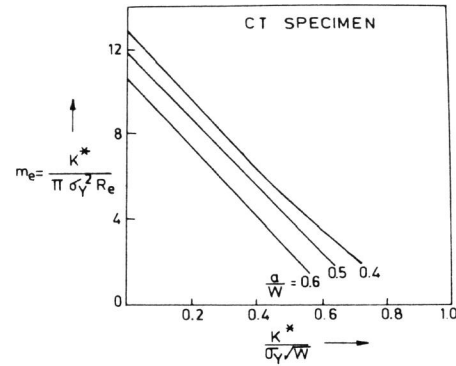


Fig. 2. Dependence of plastic zone size,  $R_e$ , on  $W$  and ' $a$ ' of CT specimen.

**Plastic Flow Curve**

The load versus load-line displacement test records were determined in CT specimen of different width and thicknesses - all with  $a/W$  of 0.5 and in tests where crack extension is absent. Due precaution was taken to ensure specimen alignment and minimize friction at the clip gauge supports and the pins during these tests. The plastic flow curves are reported in Fig. 3, where  $\Delta V_p$  is the displacement produced by growth of plastic zone and  $V_e$  is the elastic component of the displacement. In Fig. 3 the specimens are designated by their dimensions - the numbers following the letters B and W respectively indicate the thickness and the width in inches. The reason for the difference in the plastic flow curve of the specimens B1W2 and B0.5W2 and the observed scatter is discussed elsewhere (Banerjee, 1981). The results show that thickness has a small effect on the plastic flow curve. On the other hand, the plastic flow curve when plotted in terms of the parameters  $K_I / \sigma_y \sqrt{W}$  and  $\Delta V_p / V_e$  is practically independent of  $W$  even for large scale yielding as reported elsewhere (Banerjee, 1981). The agreement between the analytical and experimental plastic flow curves is good. In addition, Fig. 3 gives another important result: the 5% secant is equivalent to  $\Delta V_p / V_e = 0.05$ , and, the corresponding value of  $K^* = K_y$ . This result would be used subsequently in the new procedure of determination of fracture toughness.

The analytical and experimental plastic flow curve for mode III loading of a circumferentially cracked round bar is reported in Fig. 4. (Gupte and Banerjee, 1984). The experimental plastic flow curve is determined in specimens of 6, 12 and 22 mms diameter bars, all with  $a/D = 0.2$ . All the experimental plastic flow curves fall within the band shown in Fig. 4. Here  $\tau_y$  is the shear yield strength; and  $D$  the diameter of the bar is

analogous to the width dimension of mode I;  $\theta_{crack}$  is the twist angle produced due to the introduction of the crack, and  $\Delta \theta_p$  is the twist angle produced by the growth of plastic zone. The reasons for the scatter in the experimental results is discussed elsewhere (Gupte and Banerjee, 1984). The good agreement between the analytical and the experimental plastic flow curves in Fig. 4 confirm the general trend of size dependent plasticity observed in the case of mode I loading.

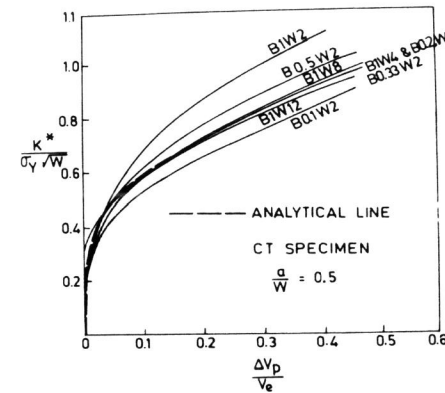


Fig. 3. Comparison of the experimental plastic flow curves from specimens of different sizes and the analytical plastic flow curve.

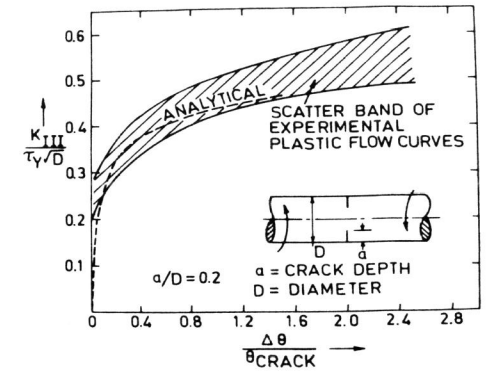


Fig. 4. Comparison of experimental and analytical plastic flow curves obtained from circumferentially cracked round bars subjected to mode III loading.

**Near Tip Contraction**

The on-load contraction at points near the crack tip has been measured using LVDT in specimens of different thickness and width. Figures 5 and 6 (Banerjee, 1981) report the  $K$  versus on-load contraction measured at 1.5 mm ahead of the crack with a straight crack front. As shown in Fig. 5 at values of  $K < K_Q$  the thickness has only a marginal effect on the contraction per unit thickness. However, at higher  $K$  values, the contraction per unit thickness increases as thickness decreases. And finally, at higher  $K$  values, the contraction per unit thickness is larger in thinner specimen ( $B = 2.5$  mm) as compared to that in the thicker one ( $B = 25$  mm).

On the other hand, as shown in Fig. 6, the effect of width on contraction is quite dramatic. In general, at higher  $K$ -values, the contraction is much less in a wider specimen ( $W = 304$  mm) compared to that in the narrow one ( $W = 50$  mm). The contraction measurements confirm the general trend of results as regards the effect of  $B$  and  $W$  on the plasticity as measured from the load-displacement test record. A lower contraction in a wider specimen indicates a small plastic zone and a higher

constraint. These aspects are also related to the reversible contraction which is discussed elsewhere (Banerjee 1981).

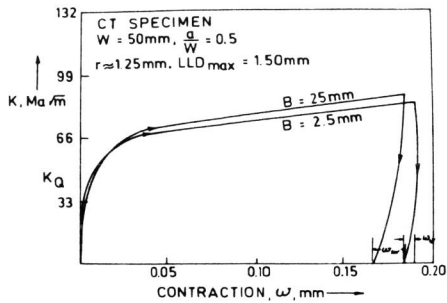


Fig. 5. Effect of thickness on contraction at 1.25 mm ahead of the crack front.

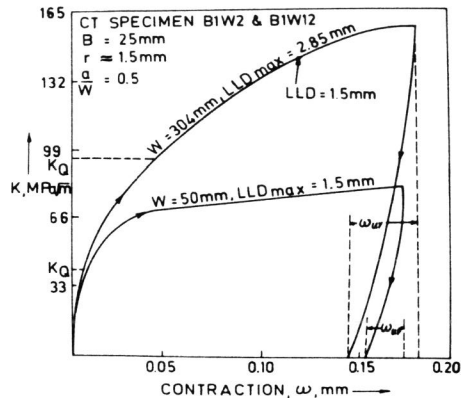


Fig. 6. Effect of width on contraction at 1.5 mm ahead of the crack front.

K<sub>Q</sub> Values

Fig. 7 reports  $K_Q^2/\sigma_Y^2 W$  versus B for two different steels. It is obvious from Fig. 7 that even a ten fold change in thickness produces only a small decrease (less than 10%.) in the  $K_Q^2/\sigma_Y^2 W$  values and for all practical purpose it can be presumed that  $K_Q$  is independent of thickness. The  $K_Q$  values reported in Fig. 7, are all determined in the absence of crack extension, and the value of  $K_Q^2/\sigma_Y^2 W$  is 0.25 for the two steels with widely differing yield strengths. As would be discussed below,  $K_Q^2/\sigma_Y^2 W = 0.25$  for all materials.

From the plastic flow curve reported in Figs. 1 and 3, it can be seen that for a  $\Delta V_p/V_e = .05$ , the corresponding  $K^*/\sigma_Y \sqrt{W} = 0.5$ , or in other words  $K^2/\sigma_Y^2 W = .25$ . Since  $\Delta V_p/V_e = .05$  corresponds to 5% secant, therefore,  $K^* = K_Q$  and so  $K_Q^2/\sigma_Y^2 W = .25$ . Thus for a CT specimen with  $a/w = 0.5$ , the plot of  $K_Q^2/\sigma_Y^2 W$  versus W should yield a straight line, which passes through the origin and has a slope equal to 0.25 (see Fig. 8). This straight line is referred to as line A in the subsequent discussion and it represents the growth of plastic zone in the absence of crack extension.

Figure 8 shows the experimental  $K_Q$  values obtained from CT specimens with  $a/w = 0.5$  prepared from different materials,

where crack extension is absent at  $K < K_Q$ . The agreement between the analytically predicted line A and the experimental  $K_Q$  values is good. This confirms that the width dependence of plastic zone and plastic constraint as predicted by the analysis, is essentially correct and applies to all materials.

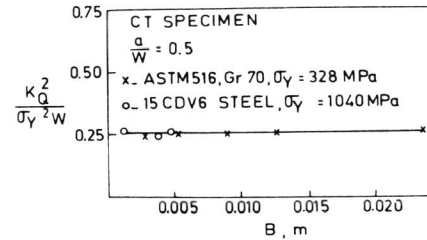


Fig. 7. Effect of thickness on experimental  $K_Q$  values.

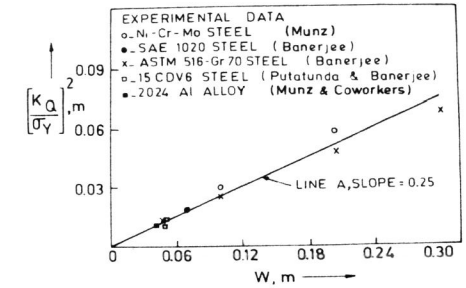


Fig. 8. Effect of width on experimental  $K_Q$  values - gives a unique line A for all materials.

Plastic Zone Size

The plastic zone size was measured by observing the out of plane contraction with the help of microscopes on the surface of both sides of 4 mm thick specimens, 25 and 200 mm wide - all with  $a/w = 0.5$ . The measurements were made with a precision of better than  $\pm .02$  mm. Even though such plastic zone size measurements are relative and are confined to the surface, the main conclusions drawn are not affected by these limitations as discussed below.

Figure 9 shows that a change in thickness from 1 to 4 mm has little effect on the plastic zone. However, one can argue that at the surface of both 1 and 4 mm thick specimens, plane stress condition exists and, therefore, plastic zone is expected to be identical; whereas the plastic zone at the interior of the 1 and 4 mm thick specimens could be substantially different. On the other hand, such an argument is inconsistent with the experimental observation that  $K_Q$  is independent of B, as reported in Fig. 7. This is explained below.

In the absence of crack extension,  $K_Q$  determined on the basis of 5% secant deviation, corresponds to a displacement which is produced by the growth of plastic zone. A simple manipulation of the compliance function together with Irwins concept of plastic zone correction factor show that, if  $K_I$ , W,  $a/w$  and the secant deviation are constant, then the plastic zone size should also be constant (Putatunda and Banerjee, 1984). Since  $K_Q$  represents the average behaviour of both 1 and 4 mm thick specimen across their respective thicknesses, a constant  $K_Q$  indicates that the overall plastic zone size across the whole

thickness of 1 and 4 mm thick specimens should be almost the same. It thus appears that at least in case of CT specimens, the effect of thickness on plastic zone is too small to be detected, as long as the plastic zones are small. These results are also supported by the effect of thickness on plastic flow curve as reported in Fig. 3.

The investigations on the effect of width on plastic zone are very limited and they are discussed elsewhere (Putatunda and Banerjee, 1984a). Figure 10 shows that at a given  $K_I$ ,  $\sigma_Y$  and  $a/W$ , plastic zone size,  $R$ , decreases as  $W$  increases. This observation is supported by the measurement of on-load contraction reported in Fig. 6. In addition, it is also supported by the observation that in the absence of crack extension,  $K_Q$  increases with width at a rate higher than one would expect from a simple calculation based on the compliance relationship and Irwin's plane strain plastic zone correction factor.

Since thickness has a relatively small effect on plastic zone and since plastic zone size decreases with increasing width, brittle crack initiation can occur in a wide plate even if the plate is thin. This explains why brittle fracture is often observed in thin but wide structures made of materials which are relatively ductile. Accordingly, this point should be taken into account in designing against brittle fracture and also in fracture toughness testing.

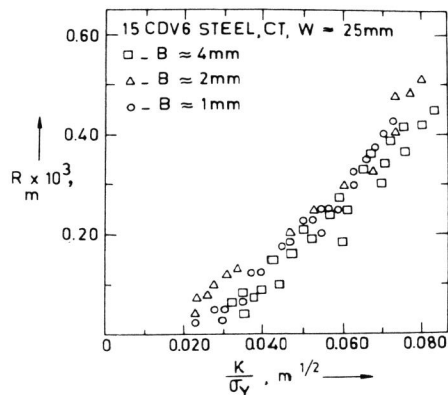


Fig. 9. Effect of thickness on plastic zone size,  $R$ .

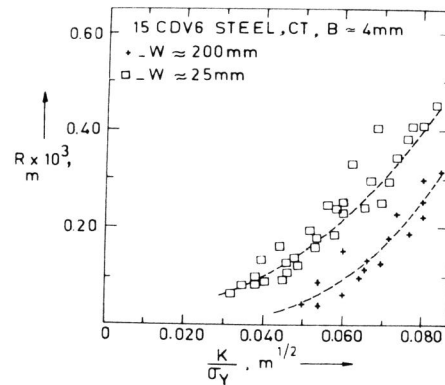


Fig. 10. Effect of width on plastic zone size,  $R$ .

#### DETERMINATION OF FRACTURE TOUGHNESS

In recent years some anomalies have surfaced which question the very basis of ASTM E399, the standard procedure for the determination of  $K_{IC}$ . For example,  $K_Q$  is observed to systematically increase with width whereas contrary to expectation,

$K_Q$  depends albeit mildly on the thickness of a CT specimen. These anomalies partly originate from the very manner in which  $K_{IC}$  is defined and determined and partly from the questions concerning the applicability of small scale yielding assumption in fracture toughness testing as given in ASTM E399.

As discussed earlier, thickness has only a small effect on plastic zone size. Therefore, the assumption that thickness increases plastic constraint and consequently promotes brittle crack initiation in CT specimen in ASTM E399 type of tests is questionable. Thickness may influence stable crack growth or unstable crack extension but these are outside the scope of ASTM E399. If fracture toughness were to, truly represent material behaviour, it must be independent of size; or, in other words,  $K_{IC}$  should be independent of dimension such as thickness, crack length and width. The fact that  $K_Q$  depends on  $W$  and 'a', raises serious doubts if one can obtain  $K_{IC}$  in specimens which have  $W$  and 'a' values larger than that required to obtain valid measurements as per ASTM E399; particularly, in a material which exhibits type I load-displacement behaviour with a rising R-curve.

There is another important aspect. ASTM E399 defines fracture toughness based on 5% secant deviation  $K_Q$ , which corresponds to 2% effective crack extension in a CT specimen with  $a/W=0.5$ . The effective crack extension is the sum of half the plastic zone and physical crack extension. Thus  $K_Q$  corresponds to an arbitrary amount of physical crack extension which ranges from 0 to 2%; the actual amount of physical crack extension at  $K_Q$  depends on the size, geometry and material and therefore could vary from one test situation to another rendering the very definition of toughness in ASTM E399 questionable. And in relatively tougher material where  $K$  rises rather sharply with increasing physical crack extension,  $K_Q$  and therefore, in some instances  $K_{IC}$  measured according to ASTM E399 would be different for different size and geometry.

#### A New Procedure of Determination of Fracture Toughness

In order to overcome the above difficulties, a new procedure of determination of  $K_{IC}$  has been described in a recent publication (Banerjee, 1981). This approach differs from ASTM E399 in two respects. First, it is based on the observation that the constraint to yielding increases and the plastic zone size decreases as the width of a CT specimen increases and secondly,  $K_{IC}$  is defined as the stress intensity factor at which crack extension starts. In the new procedure, the start of physical crack extension is identified by using a simple graphical construction.

The new approach to  $K_{IC}$  determination consists of finding out the intersection of plastic flow and crack growth resistance curves. Both these curves are analytically generated (Banerjee, 1981). For a CT specimen with  $a/W = 0.5$ , the plastic flow curve which represents growth of the plastic zone only, gives

rise to line A (Fig. 8). The line A is uniquely defined since it passes through the origin and has a slope of 0.25 in a plot of  $K_Q^2/\sigma_Y^2$  versus  $W$ . The crack growth resistance curve which represents the simultaneous growth of the plastic zone and the crack, gives rise to line B. The line B for a CT specimen with  $a/W = 0.5$ , has a slope of 0.05 in the  $K_Q^2/\sigma_Y^2$  versus  $W$  plot but this line could lie anywhere depending upon the  $K_Q$  value at which crack extension starts. The position of line B, therefore, is fixed by the experimental determination of  $K_Q$  in a specimen of adequate width, where crack extension occurs at stress intensity less than  $K_Q$ . The intersection of line A and line B obviously gives the stress intensity factor at which crack extension starts. And, this gives the fracture toughness of the material according to the new procedure. The details of the new procedure are described elsewhere (Banerjee, 1981).

#### Verification of The New Procedure

The new procedure is verified by the validation of line A and line B using experimental results. Line A had been validated earlier in Fig. 8. Line B has been verified (Banerjee, 1981) from the reported  $K_Q$  data on aluminium alloy (Kauffman and Nelson; 1974, Kauffman; 1977) and titanium alloy (Munz, 1976). However, further investigation (Putatunda and Banerjee, 1984b) on 15CDV6 steel was carried out to validate line B and ascertain if the procedure can (i) give true fracture toughness of the material, (ii) be used to determine toughness with very thin and wide specimen ( $W/B \approx 55$ ) and (iii) be used to determine fracture toughness in a material which exhibits pop-in crack extension (Type II load-displacement test record in ASTM E399).

The true fracture toughness of the 15 CDV6 steel in two heat treated conditions - designated as condition A and condition B, was determined by a laborious but unambiguous procedure. The fracture toughness specimen of various sizes were prepared from a given material and loaded to progressively higher stress intensity levels, fractured open in liquid nitrogen and subsequently their fractured surfaces were examined for evidence of crack extension. The minimum  $K_I$  value at which crack extension starts could then be identified and this gives true fracture toughness of this material. Special precaution and specimen modifications were used by Putatunda and Banerjee (1984a), to prevent out of plane bending during the loading of specimens with high  $W/B$  values. The plate was too thin to obtain valid ASTM E399  $K_{IC}$ . And since pop-in crack extension occurred,  $J_{IC}$   $K_R$ -curve standard test procedures are also not applicable. The investigation of the applicability of the new test procedure to this material is, therefore, interesting.

The  $K_Q$  values reported in Figs. 11 and 12 are in excellent agreement with the analytically predicted line B and indeed validate the new procedure. Also, the new procedure gives  $K_{IC}$  values which agree quite well with the true fracture toughness value of the materials (Putatunda and Banerjee, 1984b).

According to the analytical results (Banerjee, 1981) on plastic flow and crack growth, the line B in a plot of  $K_Q^2/K_{IC}^2$  versus  $w/w_c$  should have a slope of 0.21, for CT specimen with  $a/w=0.5$ ; where  $w_c$  is the critical width at which  $K_Q = K_{IC}$ . The analytical results predict that line B in such a plot, should be independent of the material and the experimental  $K_Q$  data of different materials plotted in Fig. 13 indeed confirm this prediction. Each  $K_Q$  data reported in Fig. 13 is the average of two to five tests and the reported  $K_Q$  values are obtained from specimens of widely varying thicknesses. Part of the scatter observed in Fig. 13 originates from the fact that  $a/w$  of the specimens tested are not equal to 0.5 in all cases. Figure 13 proves that the new procedure applies to all materials.

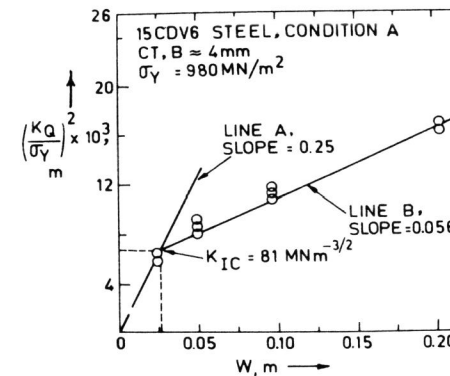


Fig. 11 Effect of width on experimental  $K_Q$  for condition A material

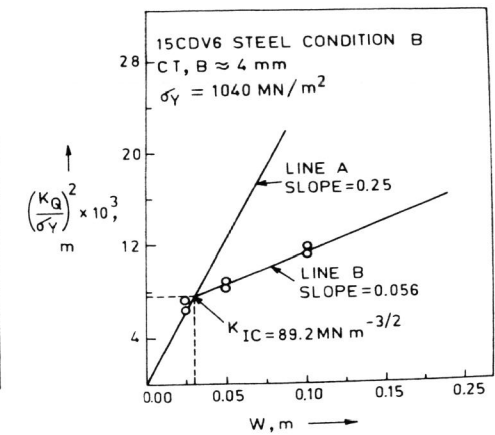


Fig. 12 Effect of width on experimental  $K_Q$  for condition B material.

#### An Appraisal of the New Procedure

From the above discussion, one can make a few important points about the new procedure of  $K_{IC}$  determination. First, the new procedure gives fracture toughness of the material which is independent of specimen width. Second, the new test procedure is identical to and, therefore, is as simple as ASTM E399 test procedure, where a single specimen is tested without taking recourse to elaborate instrumentation. Third, unlike ASTM E399,  $K_{IC}$  could be determined according to new procedure even with thin specimen. Fourth, unlike ASTM E399 where  $K_{IC}$  corresponds to an arbitrary amount of crack extension which could range anywhere from 0 to 2% depending on the material tested, the new procedure determines  $K_{IC}$  at the start of crack extension. Thus,  $K_{IC}$  determined according to the new procedure is consistent with the fundamental definition of fracture toughness and operational definition of  $J_{IC}$  and  $\delta_C$ . Fifth, the new procedure determines the true fracture toughness of a material, wherein

the start of crack extension is identified by using a simple graphical construction. This is unlike the  $J_{IC}$  or R-curve approaches, where the start of crack extension is identified by either multiple specimen technique or through elaborate instrumentation. Sixth, the new procedure can give true fracture toughness of a material which exhibits pop-in behaviour and to which other procedures of fracture toughness determination are inapplicable. Finally, the procedure establishes the scope of applicability of K-based fracture mechanics to predict linear elastic crack initiation in thin and wide structures.

Notwithstanding the points made above, the new procedure requires verification through tests with specimens of  $a/W$  other than 0.5 and geometries other than CT.

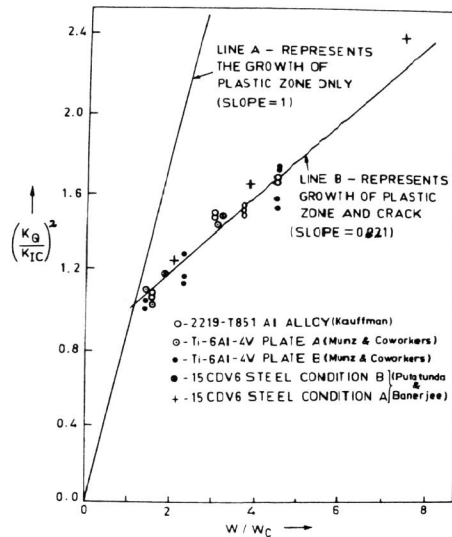


Fig. 13 Experimental and predicted results on the  $(K_Q/K_{IC})^2$  versus  $W/W_C$  plots - gives an unique line B for all materials

The results discussed thus far, concern the problems relating to the determination of a meaningful  $K_{IC}$  and the initiation of brittle fracture in thin and wide structures. In the subsequent part of the paper, the import of size and geometry dependent plasticity on studies related to fatigue crack growth rate (FCGR) is briefly discussed.

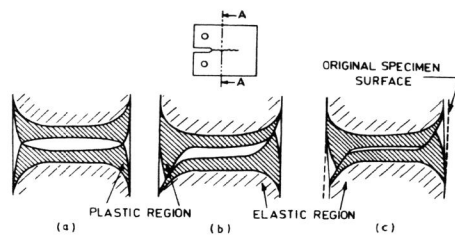


Fig. 14 Fracture surface profile as influenced by specimen size and loading (a) symmetric (b) non-symmetric profile and (c) out of plane sliding in thin specimens with non-symmetric profile, relaxes compressive force.

## FATIGUE CRACK GROWTH RATE

The problems relating to a reliable characterization of crack growth rate are briefly discussed under two subheadings: (i) an examination of fatigue crack growth rate and closure (ii) plastic energy dissipation.

### An Examination of FCGR and Closure

To predict life of a component, several empirical laws which characterize fatigue crack growth rate have been proposed. However, most of these are either derived from or are a variation of the Paris convention which states that

$$\frac{da}{dN} = A \Delta K^n \quad (2)$$

The above relationship is considered to be independent of size and geometry. Therefore, A and n determined from a test specimen made from a given material, can be used to calculate the fatigue life of a precracked structure made from the material. The above relationship, however, holds true only for constant amplitude loading and fails to account for the effects of, load ratio, R, the short crack behaviour or the overload retardation produced during variable amplitude loading. The concept of closure has been used to account for the effect of these factors on fatigue life. Accordingly, one defines an effective  $\Delta K$  which is given by  $\Delta K_{eff} = (K_{max} - K_{op})$ , and equation (2) is modified to

$$\frac{da}{dN} = A \Delta K_{eff}^n \quad (3)$$

where,  $K_{op}$  is the minimum stress intensity factor at which a fatigue crack is fully open during loading. Some investigators show that equation (3) satisfactorily accounts for the effect of R, the variable amplitude loading and the short crack behaviour, whereas the results of others do not do so.  $K_{op}$  is also related to account for the effect of residual stress, environment and change in microstructure, on FCGR. All these aspects are examined in a recent review (Banerjee, 1984a).

Several mechanisms of closure have been proposed and amongst these plasticity induced closure mechanism is better established. According to such a mechanism, the plastic flow at the crack tip leaves a strip of yielded material behind the crack tip. This is referred to as the plastic wake. Extension of the material within the plastic wake is accommodated by the rest of the precracked body which is elastic and this produces reactive compressive stresses over the crack faces. These compressive stresses keep the crack closed which is called crack closure. The introduction of residual compressive stresses and displacement in the wake of the crack alters the stress field ahead of the crack. The rationale for Paris law is that K characterizes the stress field and, therefore, relates to  $da/dN$ . However, since stress field is altered by closure, the  $da/dN$  should relate to  $\Delta K_{eff}$ , rather than to  $\Delta K$ .

A few observations as regards the effect of  $a/W$ , width, thickness and specimen geometry on  $K_{op}$  and FCGR would be appropriate



in this context.

If one takes into account results presented earlier that plastic zone size increases with increasing  $a/W$  and decreasing  $W$ ,  $K_{op}$  should correspondingly exhibit a dependence on  $W$  and  $a/W$ . Indeed, it has been observed that  $K_{op}$  is independent of  $a/W$  at intermediate  $a/W$  values; but at higher  $a/W$ ,  $K_{op}$  decreases (Paris and Hermann, 1981, Banerjee, 1984b). The effect of  $W$  on  $K_{op}$  has not been systematically investigated.

As usually assumed, if plastic zone size were to be independent of  $a/W$  and  $W$ , the plastic zone size and the spread of the plastic wake in the direction perpendicular to crack plane, would be same for all  $a/W$  and  $W$  values. Thus, at constant  $R$  and  $K_{max}$ , the spread of the plastic wake remains constant but its length increases with  $W$  and  $a/W$ . Since closure originates primarily from the wedging action of the plastic wake, a change in the ratio of the spread and the length of the wake would affect  $K_{op}$ . In addition, the finite element analysis of closure (Newman, 1982) takes into account the significant contact stress which are distributed along the crack line. The distribution of these contact stresses should change with  $a/W$  and  $W$  and this in turn can influence  $K_{op}$ . Further analytical and experimental investigations are necessary to ascertain the effect of  $a/W$  and  $W$  on closure. It must be recalled that  $K_{op}$  has been observed to depend rather sensitively on the history of loading (Banerjee 1984b); by history of loading, one means the variation of  $K_{max}$  with  $a/W$ , even in a constant amplitude FCGR test. Such dependence is often ignored in closure studies and must be taken into account in all experimental investigation of the effect of  $a/W$  and  $W$  on closure and FCGR.

The effect of thickness on  $K_{op}$  requires three-dimensional elastic-plastic analysis since, (i) fatigue crack front is curved, (ii) fatigue crack in the mid-thickness region of the specimen is in the plane of crack but near the surface layers the fatigue crack extends out of the plane of crack - both above and below it and (iii) the yielding of the specimen occurs preferentially in the surface layers. Indeed, the true nature of the three dimensional crack front is quite complicated as evident from Fig. 14. (Marci and Packman, 1980). As a result, some out of plane bending (see Fig. 14c), as also mode II and mode III, are often produced at the crack front and the magnitude of these can vary, not only with size and geometry but even between two identical specimens, or between one set of cycles to another in the same specimen. To what extent, this has produced the inconsistencies, contradictions, and scatter customarily observed in FCGR data, is hard to say.

Closure depends on formation of plastic zone and as has been shown, this depends on size and geometry. Therefore, closure and consequently, FCGR could be influenced by size and geometry. Thus,  $\Delta K_{eff}$  in case of two specimens with different size or geometry could be different even though they are loaded identically in terms of  $K_{max}$  and  $K_{min}$ . This gives rise to an inconsistency. For example, previously reported experimental

results show that equation (2) is independent of size and geometry. Therefore, if equation (3) were to be really independent of size and geometry, then this equation would be inconsistent with previously reported experimental results.

In the usual log-log representation of FCGR data as per Paris convention, a scatter band of 2 is often observed and is considered customary. Such a large scatter band is undesirable since it increases the uncertainties in the component life predicted from such data. It is likely that size and geometry has a systematic effect on FCGR due to closure and this contributes to the observed scatter band. Accordingly, the data when reported in terms of equation (3) would decrease the scatter. However, some of the evidences reported in the literature is quite the contrary.

For example, there is evidence in the literature that  $K_{op}$  in CCT is higher than that in a CT specimen (Tanaka, Matsuoka, Schimdt and Kuna, 1981). This is indirectly supported by two observations: (i) the plasticity induced closure can produce entirely different patterns of residual stresses (Banerjee, 1984a) and (ii) as discussed earlier, the plastic zone in a CCT specimen is expected to be larger than in a CT specimen. On the other hand,  $da/dN$  at a given  $\Delta K$  is higher in a CCT as compared to that observed in a CT specimen (Rhodes and Radon, 1982). Thus, if the FCGR data were to be represented in terms of equation (3) instead of (2), the scatter would increase!

On the basis of the above discussion, one can surmise that even though Paris convention is an excellent means of approximately representing FCGR data it may not satisfactorily represent the effects of secondary variables on FCGR, even when one takes into account crack closure. Several alternative procedures of representation of FCGR are being investigated and one of these is the plastic energy dissipation.

#### Plastic Energy Dissipation

When a precracked body is loaded and then unloaded, the elastic energy is fully recovered. The plastic energy dissipated (PED) during such loading is represented by  $u_p$ , and is calculated in the following manner.

$$u_p = u_t - u_e$$

where

$$u_t = \frac{1}{B} \int P \cdot dV$$

$$u_e = \frac{P \cdot V_e}{2B} = \frac{K^2 W f(a/W)}{2E [F(a/W)]^2}$$

$$f(a/W) = \text{compliance function} = E \cdot V_e B / P$$

$$F(a/W) = K \text{ calibration factor} = KB \sqrt{W/P}$$

and  $V$  is the load line displacement and consists of elastic displacement,  $V_e$ , and the displacement produced by the growth

of plastic zone,  $\Delta V_p$ . The procedure for calculation of  $V$  is reported elsewhere  $p$  (Banerjee, 1981). Apart from PED one can also compute the parameter, plastic energy dissipation rate (PEDR) which is given by  $U_p$ , where

$$U_p = \frac{\partial u_p}{\partial a}$$

Fatigue crack growth rate should relate to PED and PEDR. However, calculations show that both PED and PEDR depend on the size and geometry. Figure 15 reports the effect of  $W$ , and 'a', in addition to the effects of  $K$ ,  $\sigma_Y$  and  $E$  on PED in CT specimens.

PED can be experimentally determined using a simple operational amplifier circuit (Srikanth, 1983) or by processing numerically the digitized load-displacement test record in a computer. A typical P-V plot and the corresponding P- $\Delta V$  plot obtained through the amplifier circuit, is reported in Fig. 16 (Srikanth, 1983), where  $\Delta V = V - V_e$ . PED can be conveniently determined from the loop area of the experimental P -  $\Delta V$  plot. The magnification of  $\Delta V$  is 6 times that of  $V$ . It should be noted that the P -  $\Delta V$  plot also yields  $K_{op}$  data. Eventhough, there are inherent uncertainties in the determination of PED from the loop area, these uncertainties decrease substantially at high  $K_{max} / \sigma_Y$  and low  $R$  values.

Table 1 reports the experimental  $u_p$  values. Table 1 also reports the analytical  $u_p$  values calculated from the results reported in Fig. 15, where  $K$  is assumed to be equal to  $(K_{max} - K_{op})$ . This assumption is justified on the premise that plastic energy dissipates only when the crack is fully open. Also while calculating  $u_p$  from Fig. 15,  $\sigma_Y$  is assumed to be equal to twice the tensile yield strength of the material investigated, since the material at the crack tip undergoes reversed yielding.

The agreement between the experimental and the analytical results are good to a first approximation and are encouraging. However, if PED or PEDR were to control FCGR, then one would expect  $da/dN$  to depend on  $W$  and  $a$ . Experimental investigation of  $W$  and  $a$  on the FCGR does indicate some trends (Gupta, 1982) but it is difficult to determine the operational relationship between  $da/dN$  and  $u_p$  (or  $U_p$ ), due to the usual scatter in the experimentally determined  $da/dN$  from one specimen to another.

It is unlikely that such scatter originates entirely from a variation in the microstructure or material behaviour. It is rather likely that the local conditions around the crack tip change from one set of cycle to another due to the complex three-dimensional loading and nature of the fatigue crack front (see Fig. 14c) and this may contribute significantly to the scatter observed. The local conditions near the crack tip may change due to misalignment and out of plane bending during loading and also due to friction at the clevis pins. Use of ball-bearing in the clevis and special fixtures which prevent out of plane bending near the crack tip, may mitigate the problem.

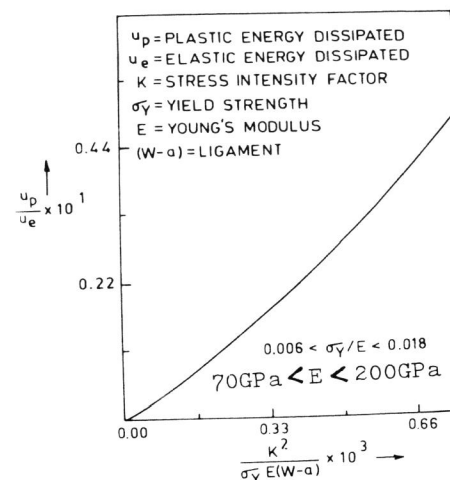


Fig. 15 Dependence of plastic energy dissipation on  $\sigma_Y$ ,  $E$ ,  $a$ ,  $K$  and  $W$  of CT specimens.

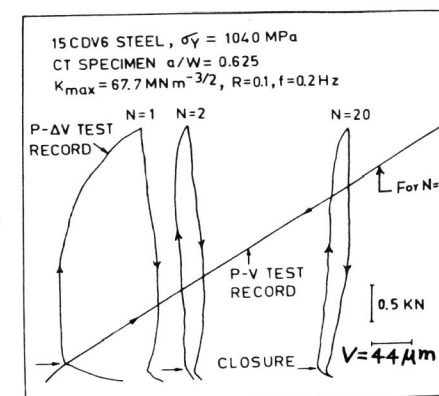


Fig. 16 Load versus offset displacement (P- $\Delta V$ ) plots for cycles,  $N = 1, 2$  and  $20$  after precracking at  $K_{max} = 20 \text{ MPa}\sqrt{\text{m}}$ .

Further investigation should be undertaken to resolve the points made above.

#### CONCLUDING REMARKS

The size and geometry of a precracked body has significant effect on plasticity. By taking these effects into account, the observed anomalies in fracture toughness testing has been resolved and a new procedure of fracture toughness determination has been developed. Plastic energy dissipated at the crack tip is size and geometry dependent; the effect of this observation on FCGR needs further examination.

Table 1. Comparison of analytical and experimental plastic energy dissipation,  $u_p$ , for  $N = 2$  cycles after precracking at  $K_{max} = 20 \text{ MPa}\sqrt{\text{m}}$ . CT specimen.  $a = 50 \text{ mm}$ ,  $R = 0.1$  and  $f = 0.1 - 0.2 \text{ Hz}$ .

| Material  | a/w   | $K_{max}$<br>MPa $\sqrt{\text{m}}$ | $K_{Op}$<br>MPa $\sqrt{\text{m}}$ | Experimen-<br>tal $u_p$<br>J/m | Analyti-<br>cal $u_p$<br>J/m |
|---|-------|------------------------------------|-----------------------------------|--------------------------------|------------------------------|
| 15CDV6 steel<br>$\sigma_Y = 1040 \text{ MPa}$   | 0.6   | 40.1                               | 10.4                              | 0.38                           | 0.32                         |
|   | 0.625 | 67.7                               | 8.5                               | 2.65                           | 3.15                         |
| Maraging steel<br>$\sigma_Y = 780 \text{ MPa}$  | 0.4   | 40.5                               | 5.6                               | 0.41                           | 0.37                         |
|   | 0.7   | 42.0                               | 5.4                               | 0.51                           | 0.65                         |
| Maraging steel<br>$\sigma_Y = 1720 \text{ MPa}$ | 0.4   | 40.0                               | 6.0                               | 0.09                           | 0.13                         |
|   | 0.7   | 41.5                               | 4.6                               | 0.13                           | 0.21                         |

## REFERENCES

- ASTM E399 (1981). Plane strain fracture toughness testing of metallic materials Annual book of ASTM standards, 10, 588-617.
- Banerjee, S. (1981). Influence of specimen size and configuration on the plastic zone, toughness and crack growth, Engineering Fracture Mechanics, 15, 343-390.
- Banerjee, S. (1984a). A review of crack closure in fatigue - To be published as a report of AFMNL Materials Laboratory, Wright Patterson Air Force Base, Ohio, USA - communicated to Engineering Fracture Mechanics.
- Banerjee, S. (1984b). An assessment of the effect of history of loading on closure during constant  $\Delta K$  FCGR tests (unpublished work).
- Broek, D. (1978). The crack tip plastic zone. Elementary Engineering Fracture Mechanics, Sijthoff and Noordhoff, Netherlands, 100.
- Chona, R., G. R. Irwin and R. J. Sanford (1983). Influence of specimen size and shape on the singularity - dominated zone. In J. C. Lewis and G. Sines (Ed.), Fracture Mechanics: Fourteenth Symposium - Volume I: Theory and Analysis, ASTM STP 791, I-3-I-23.
- de Wit, R. (1983). A review of generalized failure criteria based on the plastic yield strip model. In J. C. Lewis and G. Sines (Ed.), Fracture Mechanics: Fourteenth Symposium - Volume I: Theory and Analysis, ASTM STP 791, I-24-I-50.
- Dugdale, D. S. (1960). Yielding of steel sheets containing slits. Journal of the Mechanics and Physics of Solids, 8, 100-104.
- Elber, W. (1970). Fatigue crack closure under cyclic tension. Engineering Fracture Mechanics, 2, 37-45.
- Fuhring, H. and T. Seeger (1979). Dugdale crack closure analysis of fatigue cracks under constant amplitude loading. Engineering Fracture Mechanics, 11, 99-122.
- Gupta, A. (1982). The effect of specimen width on FCGR. M. Tech. Dissertation, Indian Institute of Technology, Bombay.
- Gupte, K. A. and S. Banerjee (1984). Fracture of round bars loaded in mode III and a procedure for K<sub>IIIc</sub> determination - to be shortly published in Engineering Fracture Mechanics.
- Heald, I. T., J. L. Sreek and R. S. Worthington (1979). Post Yield Fracture Mechanics. Materials Science and Engineering, 10(3), 129-136.
- Kauffman, J. G. and F. G. Nelson (1974). Fracture Toughness and slow stable crack growth, ASTM STP 553, 74-85.
- Kauffman, J. G. (1977). Development in Fracture Mechanics test methods standardization, ASTM STP 432, 3-19.
- Larsson, S. G. and A. J. Carlsson (1973). Influence of non-singular stress term and specimen geometry on small-scale yielding at crack-tips in elastic plastic materials. J. of the Mechanics and Physics of Solids, 21, 263-277.
- Wall, S. and S. C. Newman, Jr. (1984). The Dugdale model for compact tension specimen - paper presented at the sixteenth national symposium on Fracture Mechanics, sponsored by ASTM E-24 Committee, Columbus, Ohio, 15-17 August (1983).
- Marci, G. and F. F. Packman (1980). The effect of plastic wake zone on the conditions for fatigue crack propagation. International Journal of Fracture, 16, 282-295.
- Munz, D., K. H. Galda and F. Link (1975). Effect of specimen size on fracture toughness of a titanium alloy, ASTM STP 520, 219-234.
- Munz, D. (1977). Fracture toughness determination of the aluminium alloy 4475 - T7351 with different specimen sizes - DAVLA - DLR - 83 77-04.
- Munz, D. (1979). Minimum specimen size for the application of linear elastic fracture mechanics. Elastic-Plastic Fracture, ASTM STP 612, 406-425.
- Newman, S. C. Jr. (1981). A crack closure model for predicting fatigue crack growth under aircraft spectrum loading. J. R. Ong and C. M. Hudson (Ed.), Methods and Models for Predicting Fatigue Crack Growth under Random Loading. ASTM STP 746, 53-84.
- Paranjpe, S. A. (1977). Interrelation of crack opening displacement with stress intensity factor and  $\int$  Integral., Ph.D. Thesis, I. I. T., Bombay.
- Paranjpe, S. A. and S. Banerjee (1977). The K- $\int$  relationship for pre-loaded single edge notched specimens. Fracture 1977, Proceedings of Symposium ICF4, 3, 210-207.
- Paris, P. C. and P. Erdogan (1963). A critical analysis of crack propagation laws. Journal of Basic Engineering, Transaction ASME, 85, 528-534.
- Paris, P. C. and L. Hermann (1981). 'Twenty years of reflections on questions involving fatigue crack growth, Part II: Some observations of crack closure. Fatigue Threshold, EMAS Publications, Warely, U.K. 11-32.
- Putatunda, S. K. and S. Banerjee (1984a). Effect of size on plasticity and fracture toughness. Engineering Fracture Mechanics 19(3), 507-540.
- Putatunda, S. K. and S. Banerjee (1984b). Determination of fracture toughness of a material which exhibits pop-in behaviour. Journal of Testing and Evaluation, ASTM - to be published in September, 84.
- Rajendran, A. N. and S. Banerjee (1984). Finite element investigation of the effect of size and geometry - unpublished work at AFMNL Materials Laboratory, WPAFB, Ohio (USA).

- Rhodes, D. and J. C. Radon (1982). Effect of some secondary test variables on fatigue crack growth. Fracture Mechanics: Fourteenth Symposium, ASTM STP 791, II, 33-46.
- Tanaka, K. S. Matsuoka, V. Schmidt and M. Kuna (1981). Influence of specimen geometry on delayed retardation phenomenon of fatigue crack growth in AYSO steel and aluminium alloy. Proceedings of 5th International Conference on Advances in Fracture, Cannes, France, 1789-1798.
- Terada, H. (1983). Elastic and elasto-plastic stress analysis of the standard compact tension specimen. Transaction of the ASME, Journal of Pressure Vessel Technology, 105, 132-137.
- Srikanth, R. (1983). Plastic energy dissipation and crack closure studies in fatigue. M. Tech Dissertation, I.I.T. Bombay.
- Wilson, W. K. (1967). Discussion. W. F. Brown Jr. and J. E. Srawley (Ed.), Plane strain crack toughness testing of high strength metallic materials. ASTM STP 410, 75-76.